16th Australasian Fluid Mechanics Conference
Crown Plaza, Gold Coast, Australia
2-7 December 2007

An eigenmode analysis of time delays in an acoustically coupled multi-bubble system

H. Yoon[1], A. Ooi[1] and R. Manasseh[2]

[1]Department of Mechanical and Manufacturing Engineering
University of Melbourne, Melbourne, Victoria, 3010 AUSTRALIA
[2]Energy and Thermofluids Engineering, CSIRO Manufacturing and Infrastructure Technology,
P.O. Box 56, Highett, Melbourne, Victoria, 3190 AUSTRALIA

Abstract

The acoustic properties of an inhomogeneous bubbly medium are complex owing to the absorption and re-emission of acoustic energy by the bubbles. This phenomena can be approximated by a globally coupled system of linear oscillators. In previous studies, it has been shown that this simple model can produce results that are in qualitative agreement with experimental data. In order to achieve better quantitative agreement with experimental data, time-delays need to be introduced into the mathematical model.

In the present study, the resulting delayed differential equations were solved numerically using a 4th order Runge-Kutta method. The numerical methodology was validated by comparing simplified cases with the solution using analytical methods. The effects of time-delay were assessed by comparing non-time-delayed and time-delayed versions of the mathematical model. Results from numerical simulations were then compared to assess the effects and importance of the inclusion of time-delay in the mathematical model.

This study shows that the inclusion of time-delay has a noticeable effect on the lower frequency modes of the model. This effect propagates to the higher frequency modes as the magnitude of the time-delay increases. The results also shows that the time-delay shifts the dominant modes from the lower frequency modes to the higher frequency mode.

Introduction

A bubbly medium's acoustical properties are directly related to the oscillatory behaviour of individual bubbles, which are dependent on the oscillatory behaviour of all the other bubbles. This interdependent oscillatory behaviour is influenced by several highly variable factors such as the spacing and distribution of the bubbles, the size of the bubbles and the number of bubbles in the system. The changes in the acoustic properties include the liquid medium's attenuation, scattering and propagation of sound. The void fraction of bubbles needed to be added into the medium to induce a significant change in the medium's acoustic properties is less than one percent [1].

To study the acoustic behaviour of bubbly media, Foldy [2], Van Wijngaarden [3] and Caflisch et al. [4] have introduced a mathematical formulation that models the behaviour acoustic propagation in the medium. The medium is assumed to be a continuum with averaged properties. A detailed study was conducted by Commander et al. [5] on the model of Caflisch et al. [4] with various experimental data that was available at the time [6, 7, 8, 9, 10]. The analysis showed limited success of the model, with one of the major problems being that the accuracy was severely impaired once the void fraction reached 1% -2%.

Feuillade et al [11] developed another method to explain the multiple scattering and the interaction between bubbles. In this method, called the self-consistent method, individual bubbles are modelled together with their acoustic interactions, rather than using a continuum with average properties. Feuillade [12] made a comparison between the self-consistent methodology and multiple scattering methodology, showing the self-consistent methodology has an advantage in dealing with situations where there is a strong interaction between the bubbles.

Manasseh et al. [14] used the coupled oscillator model to compute the acoustic field in the vicinity of a bubble chain without time-delay. Comparison with experimental data showed that while an anisotropy in the acoustic field due to the chain was predicted, the coupled oscillator model can only reproduce the qualitative trend in the experimental data.

From the studies mentioned, one of the common assumptions inherent in the modeling of multiple scattering and interaction between bubbles is that the propagation speed of pressure perturbations (speed of sound) between the bubbles is infinite. To incorporate the finite speed of propagation of acoustic energy into the mathematical model, a time-delay is added [15] [17]. The addition of time-delays has been shown have significant effects on the overall behaviour of the mathematical model. Even when there are only two bubbles in the system, it has been shown by [16] that time-delay has a significant effects on the damping constant of the system. Doinikov at el [16] showed that time-delays could improve earlier predictions [14].

This paper will focus on the how the inclusion of the time-delay into the model can effect the behaviour of the overall globally coupled oscillator model.

Mathematical Model

A globally coupled linear oscillator model is used to represent a multi-bubble system (for scope of the present study, a bubble chain). This model is a combination of the linearized bubble oscillation model and the self-consistent methodology.

The scattered pressure field generated by a single bubble can be expressed as

$$P_n(t) = \rho \frac{R_{0m}^2}{d_m} \ddot{r}_m(t) \tag{1}$$

(see Vokurka [18]), where ρ is the density of the liquid, R_{0m} is the equilibrium radius of the mth bubble, $r_m(t)$ represents the bubble's radial deviation from it's equilibrium radius and d_m is the distance from the bubble.

The self-consistent methodology defines that the total pressure field on any bubble to be the sum of the external field plus the scattered fields from all the other bubbles [12]. Mathematically, this can be expressed as

$$P_t(t) = -\sum_{m=1}^{n} \rho \frac{R_{0m}^2}{d_m} \ddot{r}_m(t). \quad (2)$$

The dynamics of the individual bubbles in the globally coupled linear oscillator model is modelled using the linearized Rayleigh-Plesset equation [19],

$$\ddot{r}_n(t) + \omega_{n0}\delta_n \dot{r}(t) + \omega_{n0}^2 r(t) = -\sum_{\substack{m=1 \\ m\neq n}}^{N} \frac{R_{m0}^2}{R_{n0} d_{nm}} \ddot{r}_n(t), \quad (3)$$

where $r_n(t)$ represents a small radial deviation from the bubble's equilibrium radius, ω_{n0} is the resonant angular frequency of the nth bubble (Minnaert's frequency [20]), δ_n describes the total damping of the nth bubble, where $\delta_n = \delta_{nr} + \delta_{nt} + \delta_{nv}$ and δ_{nr} is the radiation damping, δ_{nt} is the thermal damping and δ_{nv} is the viscous damping (Devin [21]), R_{n0} is the equilibrium radius of the nth bubble and d_{nm} is the distance between the nth and mth bubbles.

Equation (3) has an inherent assumption that the liquid medium is incompressible, resulting in acoustic waves travelling at an infinite speed. To account for the finite speed of pressure perturbation propagation, a time-delay needs to be introduced into the model, resulting in the following second order delay differential equations,

$$\ddot{r}_n(t) + \omega_{n0}\delta_n \dot{r}(t) + \omega_{n0}^2 r(t) = -\sum_{\substack{m=1 \\ m\neq n}}^{N} \frac{R_{m0}^2}{R_{n0} d_{nm}} \ddot{r}_n(t - \frac{d_{nm}}{c}), \quad (4)$$

where c is the speed of sound.

The time-delayed globally coupled oscillator model is categorized as neutral second-order delay differential system. All delay differential systems required one additional common user-defined input when using numerical methods like the fourth-order Runge Kutta method. The additional input required is the past history of the system before the point of initial simulation (i.e. the time range of $\min(-d_{nm}/c)$ to 0). Bellen and Zennaro [22] state that the solution of the delay differential system could be very sensitive to the user defined history of the system.

Both the non time-delay equation (3) and the time-delay equation (4) are solved using the fourth-order Runge Kutta method. The time-delay equation (4) can also be solved using an iterative analytical method described in Hu et al. [23] and modified by Ooi et al. [24] to include time-delays in the highest order derivative term. Data from the two methods were compared to validate the results presented in the the paper.

The history $r_n(t)$ of the multi bubble system was set to the value of 0 in the range of $\min(-d_{nm}/c)$ to 0, this can be thought as the overall system was inactive (or at rest) before t = 0. This assumption is only needed for simulations carried out using the fourth order Runge-Kutta method, not the iterative analytical method, for in the process of solving the system analytically, the method inherently assumes a history of time < 0 which ensures a smooth function in the vicinity of t=0.

Using the iterative analytical method, the solutions to equations (3) and (4) can be expressed as

$$\vec{r}(t) = \vec{A}e^{\lambda t}, \quad (5)$$

Figure 1: Photo of the bubble chain's lower section. Reproduced from Nikolovska [25].

Number of bubbles	16	19	40	56
Bubble radius (m)	0.0035	0.0035	0.00118	0.00141
Bubble separation (m)	0.0321	0.0249	0.036	0.030
Length of chain (m)	0.4815	0.4731	1.4040	1.6500

Table 1: Experimental setting for 16, 19, 40 and 56 bubble chain case.

where $\vec{r}(t)$ is a vector composed of individual bubble radius components $r(t)_n$, $\vec{A}$ is the eigenvector corresponding to the eigenvalue λ. For differential systems of size $N \times N$, there are $2N$ eigenvalues which can be expressed as

$$\lambda = \xi + i\omega, \quad (6)$$

where ω is the natural frequency, ξ is the damping for the corresponding eigenvector (mode) and i is the imaginary unit. The eigenvalues and eigenvectors occurs in a complex conjugate pairs which means there are only N linearly independent eigenvalues and eigenvectors.

For a single bubble scenario the eigenvalue can be simplified to

$$\lambda = -\frac{\omega_0 \delta_0}{2} \pm \sqrt{\left(1 - \frac{\delta_0^2}{4}\right)}, \quad (7)$$

where natural damping is $\xi_0 = {}^{\omega_0\delta_0}/_2$, natural frequency is$\omega_{01} = \omega_0\sqrt{\left(1 - {}^{\delta_0^2}/_4\right)}$, ω_0 is the minnaert's frequency and δ_0 is the total damping of the bubble.

Experimental results

The numerical simulation will be based on the experimental studies conducted by Manasseh et al. [14] and Nikolovska [25].

Figure 1 is a picture of the configuration of the bubble chain structure from the experiment. This configuration is form when the bubbles were produced and rise naturally at a constant rate at the bottom of the water tank. This results in the bubble orientated in straight line in a vertical direction. Figure 2 is a simplified diagram of figure 1, where y is the parallel distance from the location of the first bubble along the bubble chain, x is the perpendicular distance from the first bubble and L is the total length of the bubble chain.

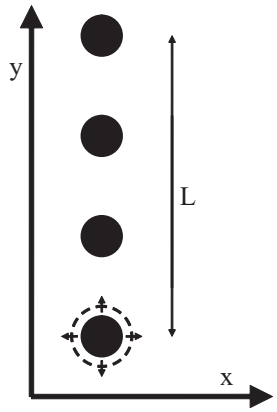

Figure 2: Simplified diagram of bubble chain arrangement.

Table 1 are the summary of the relevant experimental parameters recorded from the experimental cases, for the numerical simulation using Eqs. (3) and (4). The experimental results can be found in figure 7. These experimental results are used as the base case to both validate and also to study the effect of time-delays in the model.

time-delay analysis

Damping and mode frequency

Since the coupled oscillator model has a finite number (N) of individual oscillators, the result will be a set of N eigenmodes. The analysis of the mode damping and frequency of the globally coupled linear oscillator system is conducted using the same analysis as described in Ooi et al. [24]. Figures 3 and 5 are plots of normalized damping constant and figures 4 and 6 are the normalized mode frequency constant plots. Figures 3 to 6 are normalized by the standard second ordered differential system natural damping (ξ_0) and natural frequency(ω_{01}) and plotted against normalized separation distance between the bubbles ($y_0 = {}^{y\omega_0}/_{c}$). Every distinct line in the figures 3 to 6 represents a distinct mode of the system.

Figures 3 and 4 are generated by keeping the radius of the bubble constant and varying the bubble separation distance.

Result of the 16 bubble case is similar to the result of 10 bubble chain case in Ooi et al. [24]. The non time-delay case shows no crossover for either damping or frequency results. The time-delay case exhibits the behaviour of crossover for both damping and frequency results. The crossover for damping occurs at intervals of $y_o = 1/2$. The frequency crossover patten repeats itself over interval of $y_o = 1/2$ but depending on which two relative mode being compared, the interval of y_0 for 2 consecutive crossover various.

The figure 5 and 6 are generated by varying the radius of the bubble and keeping the bubble separation distance constant. Important point to note is that these four plots have been plotted against normalized bubble spacing(This is possible because the normalize bubble spacing is a function of Minnaert's frequency, which is function of bubble radius). The justification for this is to allow an easy comparison between the figures 3 to 6.

The comparison of figures 3 to 6 shows that the variation of the bubble radius in the bubble chain has the same effects as the variation in the bubble separation distance. The only difference to note is that the increasing in the bubble radius has same effect as decreasing the bubble separation distance. This result shows

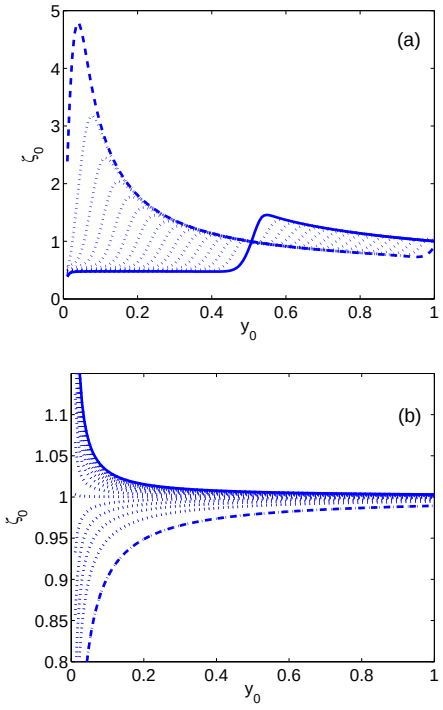

Figure 3: Plot of normalized damping for 16 bubble chain case at constant radius of 3 mm and varying bubble spacing between 7 mm to 1200 mm, where (a) is the time-delay and (b) is the non time-delay. —·— is the 1st mode, ——— is the 16th mode and ····· is mode 2nd to 15th

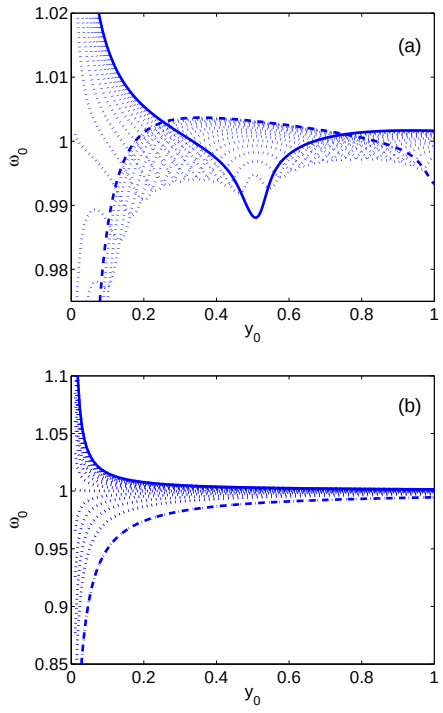

Figure 4: Plot of normalized frequency for 16 bubble chain case at constant radius of 3 mm and varying bubble spacing between 7 mm to 1200 mm, where (a) is the time-delay and (b) is the non time-delay. —·— is the 1st mode, ——— is the 16th mode and ····· is mode 2nd to 15th

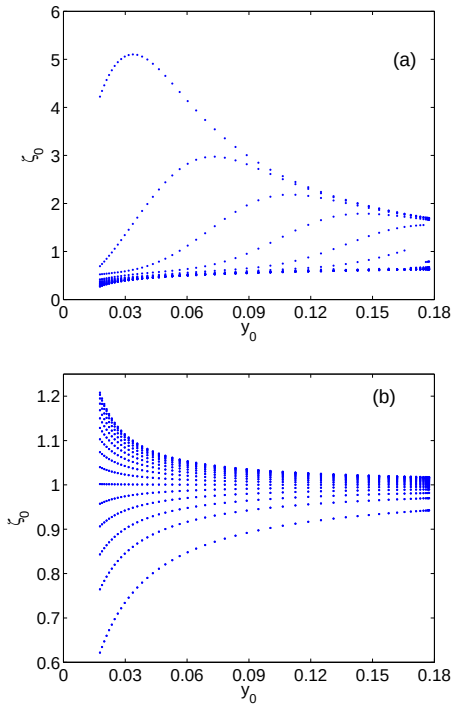

Figure 5: Plot of normalized damping for 16 bubble chain case at constant spacing of 3 mm and varying radius of 1 mm to 10 mm, where (a) is the time-delay and (b) is the non time-delay.

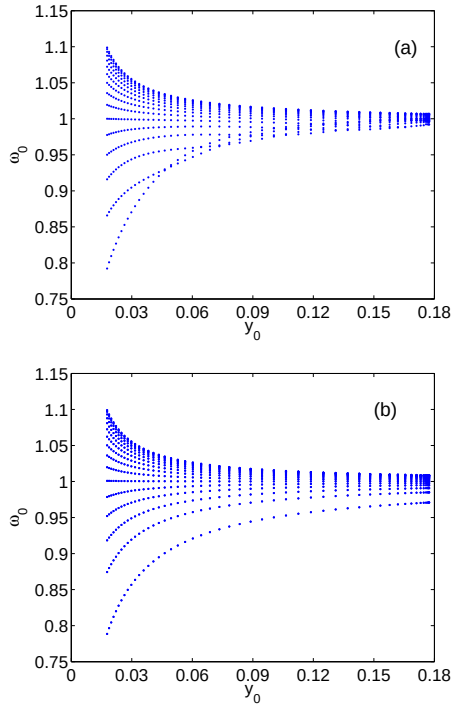

Figure 6: Plot of normalized frequency for 16 bubble chain case at constant spacing of 3 mm and varying radius of 1 mm to 10 mm, where (a) is the time-delay and (b) is the non time-delay.

that from the perspective of the damping and frequency, the effect of increasing the spacing can be negated by increasing the bubble radius.

Results and discussion

Results of this section is compilation of numerical simulation of equations (3) and (4). Results from the numerical simulations are compared with the experimental data for 16, 19, 40 and 56 bubble chain cases.

Figure 7 is the plots of normalized RMS pressure parallel to the bubble chain 6 cm away (to match the same location as in the experiments).

All the results from the numerical simulations analyzed shows the inclusion of time-delay has a very noticeable improvement in the correlation between the numerical simulation and the experimental result.

There is a clear trend in all the cases that the calculations without time-delay predict much higher RMS pressure along the bubble chain than the experimental results. In figure 7 (a) and 7 (b) the normalized RMS pressure value at the end of the bubble chain was still 0.7 to 0.8, which is much greater than what was recorded in the experimental results. Another discrepancy that can be noticed is the difference in the general behaviour of the RMS pressure profile. In both the 16 and 19 bubble chain cases, there is large decrease of RMS pressure at the first half of the bubble chain and also a slight increase in RMS pressure at the end of the bubble chain. In the 19 bubble chain case there is also a increase in RMS pressure before the decrease at the start of the bubble chain. The non time-delay model does not predict these behaviours and implies that the model maybe over simplified.

In figure 7 (c) and 7 (d), the 40 and 56 bubble chain case, the non time-delay model shows much better agreement with the experimental result than the equivalent predictions for the 16 and 19 bubble cases. The non time-delay model, predicted better initial decrease of the RMS pressure in the start of the bubble chain for the 40 and 56 bubble chain cases but the overall prediction still greater than what was recorded experimentally.

In examining of the time-delay model results, there is a fair level of agreement between the numerical results and the experimental results for all the cases studied when compare to the non time-delay case. The 16 bubble chain case shows much improved agreement, as the numerical result displays similar features, with a major decrease in RMS pressure up to the 0.2 m segment of the bubble chain and the slight rise at the end of the bubble chain exhibited by the experimental results. However, some relative magnitudes of the features are still inconsistent. The 19 bubble chain case shows less agreement as the model does not predict the initial increase in the RMS pressure before decreasing, but other than this noticeable fault there still are major improvements compared to the non time-delay model.

In the 40 and 56 bubble chain cases, the non time-delay calculation results already showed very promising results. Hence as expected with the 16 and 19 bubble chain cases, the time-delay case shows improve agreement. The predicted RMS pressure for the 40 and 56 bubble chain cases shows a similar shape to the non time-delay case, but the value predicted are lower, giving a better agreement with the experimental result.

Instantaneous pressure profile

In the experimental study of the bubble chains [14], the anisotropy property on the bubble chain was documented and this property was further explored in Nikolovksa et al. [26] by

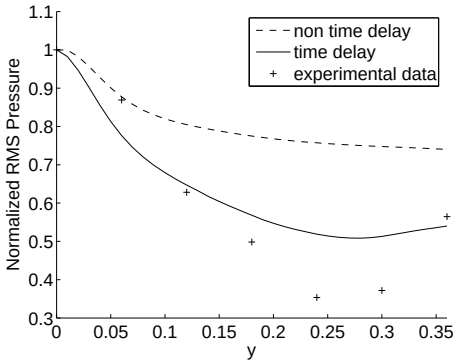

(a) 16 bubble case

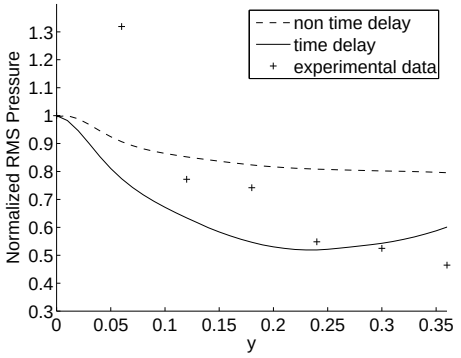

(b) 19 bubble case

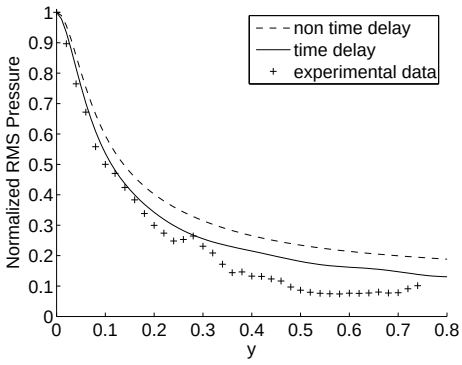

(c) 40 bubble case

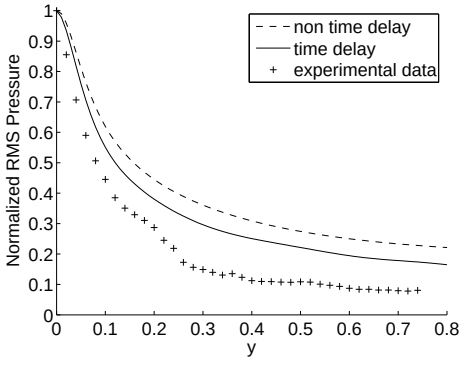

(d) 56 bubble case

Figure 7: Numerical and experimental results for 16, 19 40, 56 bubble chain case .

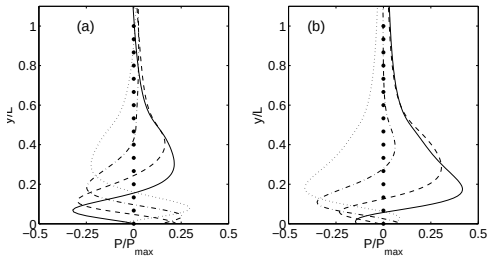

Figure 8: Energy spectra plot for time-delay 16 bubble chain case with radius 0.0035m and 0.0321m where (a) time-delay and (b) non time-delay. ——— is t = 0.036s, — — — is t = 0.038s, —·— t = 0.040s, ····· is the 0.042s and • is the location of the bubbles

measuring the instantaneous pressure along the bubble chain. These previous studies showed that wavelength of the instantaneous pressure profiles gets larger as it travels along the bubble chain and that the wavelength was in similar order of magnitude as the length of the bubble chain.

In this study the instantaneous pressure profile along the bubble chain was numerical calculated using equation (3) and (4). The results are shown in figure 8. In the plot, the instantaneous pressure is normalize by maximum instantaneous pressure to allow an easy comparison of the anisotropy property between the non time-delay and time-delay model.

Figure 8 shows both time-delay and non time-delay model display similar characteristics as in the experiments [26] with wavelength being similar magnitude to the bubble chain length. The result also shows that the wavelength of the pressure profile is longer near the end of the bubble chain compared to the start of the bubble chain.

Mode shape

This section will analyze the effect of time-delay on the global coupled oscillator system's mode shapes.

Figure 11 to 13 are the plots of first 10 mode shape, out of 16 possible mode shape from the equation (3) (non time-delay) and (4) (time-delay) for the 16 bubble chain case with separation distances of 0.0300 m, 0.0320 m, 0.0321 m, 0.0900 m and 0.1500 m. The equivalent normalize bubble separation distance for the bubble spacing are 0.01901, 0.02028, 0.02034, 0.05704 and 0.09507. The comparison between the non time-delay and time-delay mode shape plots shows time-delay has a strong effect on the low frequency modes and negligible effects on the higher frequency modes. The most noticeable differences between the modes occur up to mode 5 with mode 6 onwards only starting to show the effect of time-delay in the bubble separation case of 0.15 m. Of course, as the mode number increases for a number of bubbles, the mode shape diagram becomes rougher in appearance, since the bubble spacing is inadequate to resolve the mode structure; indeed, for a mode number greater than $N/2$, the mode shape plot will begin to be aliased.

The comparison of figures 9, 12 and 13 shows that the effect of time-delay on the system gets more noticeable as the spacing between the bubbles gets larger. As the time-delay effects becomes greater, they begin to affect the higher frequency modes more. This is expected since the time-delay constant is a function of bubble spacing. Hence an increase in the bubble spacing means increase in the magnitude of the time-delay constant.

There also seems to be a further interesting observation, com-

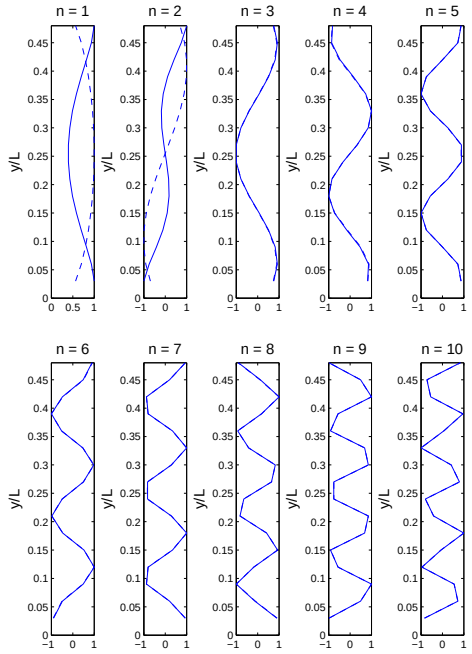

Figure 9: First 10 mode shape of Equ. (3) and (4) for 16 bubble chain with bubble radius 0.0035 m and bubble separation distance of 0.0300 m. ——— is the time-delay case and — — — is the non time-delay case

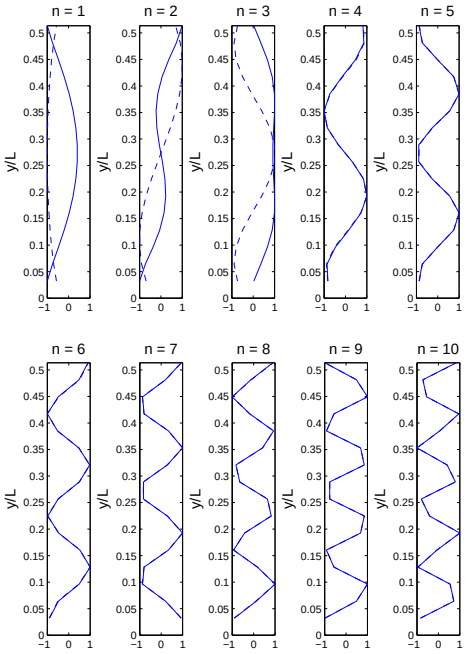

Figure 11: First 10 mode shape of Equ. (3) and (4) for 16 bubble chain with bubble radius 0.0035 m and bubble separation distance of 0.0321 m. ——— is the time delay case and — — — is the non time-delay case

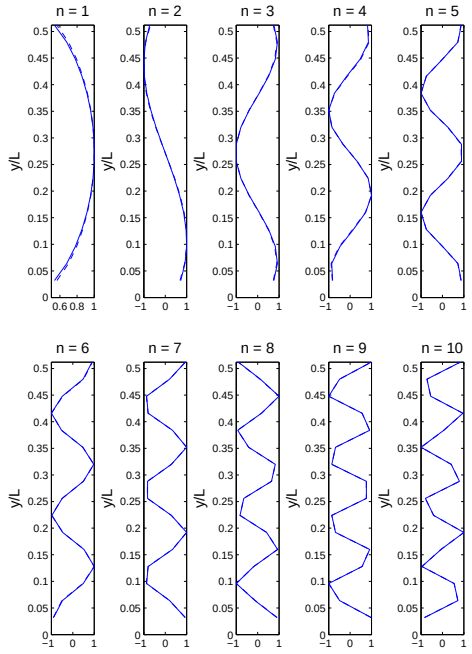

Figure 10: First 10 mode shape of Equ. (3) and (4) for 16 bubble chain with bubble radius 0.0035 m and bubble separation distance of 0.0320 m. ——— is the time-delay case and — — — is the non time-delay case

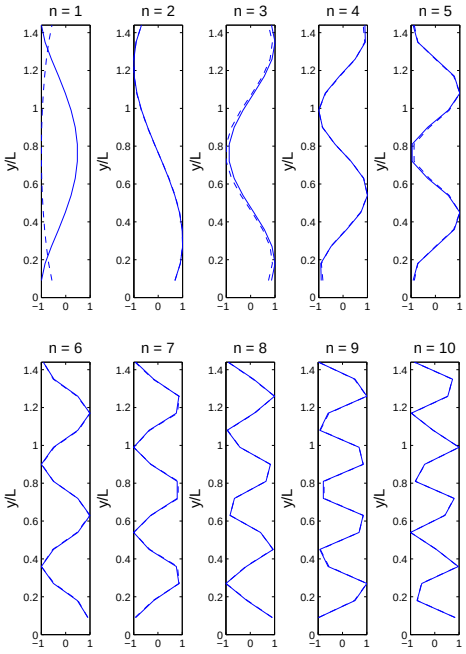

Figure 12: First 10 mode shape of Equ. (3) and (4) for 16 bubble chain with bubble radius 0.0035 m and bubble separation distance of 0.0900 m. ——— is the time-delay case and — — — is the non time-delay case

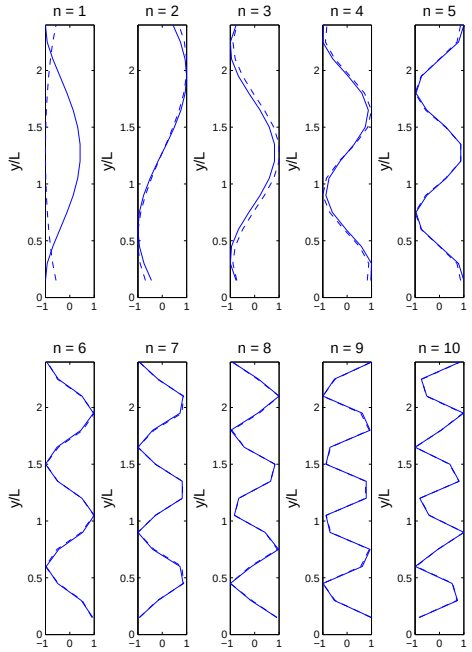

Figure 13: First 10 mode shape of Equ. (3) and (4) for 16 bubble chain with bubble radius 0.0035 m and bubble separation distance of 0.1500 m. ——— is the time-delay case and — — — is the non time-delay case

paring figures 9, 10 and 11. There is a shape changes in the mode shapes for a small change in the bubble separation distance, noticeable for the second and third modes, when the separation is around 0.0300 m. The mode shapes do not change so greatly for larger separation.

Energy spectra

This section will analyze the effect of time-delays on the energy spectra.

Figures 14 to 17 are plots of energy spectra for the non time-delay and time-delay cases. The evolution of the energy spectra in the time domain show an interesting effect that time-delay has on the system. In the non time-delay case, there is no dominant mode in the system at the start but as the model is allowed

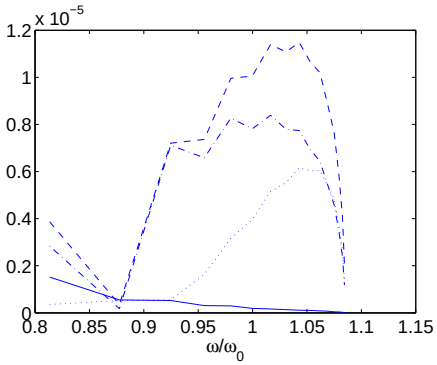

Figure 14: Energy spectra plot for time-delay 16 bubble chain case with radius 0.0035 m and spacing 0.0321 m. ——— is t = 0.000s, — — — is t = 0.0002s, —·— is t = 0.0004s and ····· is t = 0.0006s

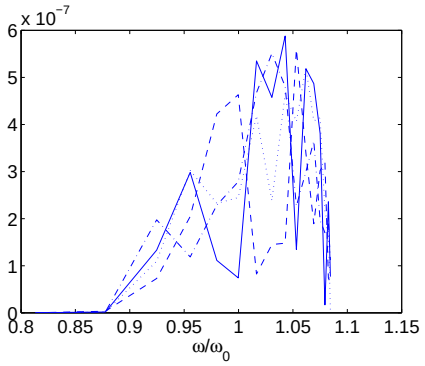

Figure 15: Energy spectra plot for time-delay 16 bubble chain case with radius 0.0035 m and spacing 0.0321 m. ——— is t = 0.0800s, — — — is t = 0.0802s, —·— is t = 0.0804s and ····· is t = 0.0806s

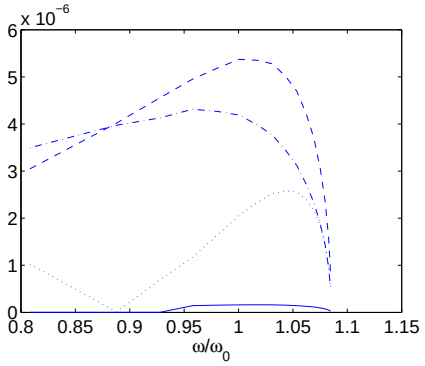

Figure 16: Energy spectra plot for non time-delay 16 bubble chain case with radius 0.0035 m and spacing 0.0321 m. ——— is t = 0.0000s, — — — is t = 0.0002s, —·— is t = 0.0004s and ····· is t = 0.0006s

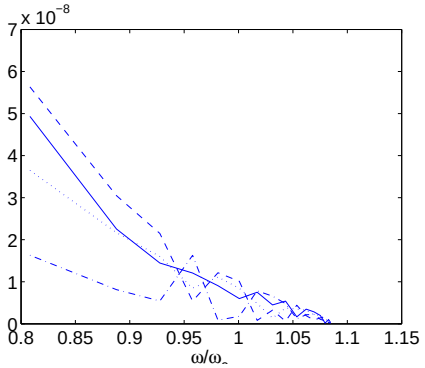

Figure 17: Energy spectra plot for non time-delay 16 bubble chain case with radius 0.0035 m and spacing 0.0321 m. ——— is t = 0.0800s, — — — is t = 0.0802s, —·— is t = 0.0804s and ····· is t = 0.0806s

to run, the higher frequency modes die out and low frequency modes starts to dominate. This was noted earlier [14] as the explanation of why experimental bubble sound pulses in frequency during the pulse when there are other bubbles nearby. In the time-delay case, there is also no dominant mode at the beginning but as the model is allow to run, first 3 mode reduces in magnitude and system is dominated by medium and high frequency modes.

Conclusion

This study illustrates the time-delay modification has shown to improve the agreement between global coupled linear oscillator model and the experimental results. The improvement does not allow the model to predict all the of the behaviours seen in the experimental results but does show that addition insight can be gained by exploring the system.

The effects of time-delay on the eigenmodes of the globally coupled linear oscillator system has been explored. The analysis looked into the mode damping and frequency, mode shapes and energy spectra. In all the cases, the effects of time-delay was noticeable with the damping and frequency results showing time-delay introduced crossovers. The mode shape analysis shows that the time-delay effect increased with increase in the bubble separation distance, and also showed a secondary feature; a sensitive dependence on bubble spacing. The energy spectra plots shows for the non time-delay case, the dominate mode of the system was the low frequency, but with the time-delay modification the dominant mode is the high frequency mode.

Bibliography

References

[1] Lu, N. Q, Prosperetti, A., Yoon, S, Underwater noise emissions from bubble clouds, IEEE J. of Oceanic Eng. 15 (4), 1990, 275-281.

[2] Foldy, L. L., The multiple scattering of waves. Phys. Rev. 67, 1945,107-119.

[3] van Wijngaarden, L., On equations of motion for mixtures of liquid and gas bubbles, J. Fluid Mech. 33, 1968, 465-474.

[4] Caflisch ,R. E., Miksis , M. J., Papanicolaou. G. C., and Ting, L., Effective equation for wave propagation in bubbly liquids. J. Fluid Mech., 153, 1985, 259-273.

[5] Commander, K. W., and Prosperetti, A., Linear pressure waves in bubbly liquids: Comparison between theory and experiments, J. Acoust. Soc. Am. 85, 1989, 732-746.

[6] Silberman, E, Sound velocity and attenuation in bubbly mixtures measured in standing wave tubes, J. Acoust. Soc. Am. 29, 1957, 925-933.

[7] Fox, F., Curly, S., and Larson, G., Phase velocity and absorption measurments in water containing air bubbles, J. Acoust. Soc. Am. 27, 1955, 534-546

[8] Kol'tsova, I., Krynskii, L., Mikhalow, I., and Pokrovskaya, I., Attenuation of ultrasonic waves in low-viscosity liquids containing gas bubbles, Akust. Zh. 25, 1979, 725-731

[9] Macpherson, J., The effect of gas bubbles on sound propagation in water, Proc. Phys. Soc. London Sec. B 70, 1957,85-82

[10] Ruggles, A., Scarton, H., and Lahey, R., An investigation of the propagation of pressure perturbations in bubbly air/water flows, in First, International Multiphase Fluids Transient Symposium edited by H. Safwat, J. Braun, and U. S. Rohaatgi (American Soceity of Mechanical Engineers, New Yorks, 1986).pp1-9

[11] Feuillade, C., Nero, R. W., and Love, R. H., A low frequency acoustic scattering model for small schools of fish," J. Acoust. Soc. Am. 99, 1996, 196-208.

[12] Feuillade, C., Acoustically coupled gas bubbles in fluids: Time domain phenomena, J. Acoust. Soc. Am. 109, 2001, 2606-2615.

[13] Ye, Z., and Feuillade, C., Sound scattering by an air bubble near a plane sea surface, J. Acoust. Soc. Am. 102, 1997, 798-805.

[14] Manasseh, R., Nikolovska, A., Ooi, A., and Yoshida, S., Anisotropy in the sound field generated by a bubble chain, J. Sound Vib., 278, 2004,807-823.

[15] Mettin, R., Luther, S., Kamphausen, S., and Lauterborn, W. Dynamics of delay-coupled spherical bubbles, in Proceedings of 15th International Symposium on Nonlinear Acoustics, Goettingen, Germany, 1-4 Sept., 1999 (AIP Melville, NY, 2000), pp. 359-362.

[16] Doinikov, A. A., Manasseh, R. and Ooi, A., Time delays in coupled multibubble systems, J. Acoust. Soc. Am., 116, 2005, 1–4.

[17] Fujikawa, S., and Takahira, H., A theoretical study on the interaction between two sphericial bubbles and radoated pressure waves om a liquid, Acustica, 61, 1986, 188-199.

[18] Vokurka, K., On Rayleigh's Model of a Freely Oscillating Bubble, I. Basic Relations, Czech. J. Phys., Sect. A, B35, 1985, 28-40

[19] T. G. Leighton, The Acoustic Bubble, 1st ed. Academic, London, 1994.

[20] Minnaert, M., On musical air bubbles and the sound of running water, Philos. Mag., 16, 1933 , 235-248.

[21] Devin, C., Survey of thermal, radiation and viscous damping of pulsating air bubbles in water, J. Acoust. Soc. Am. 31, 1959,1654-1667.

[22] Bellen, A. and Zennaro, M. Numerical methods for delay differential equations, Oxford University Press, New York, 2003.

[23] Hu, H. Y., Dowell, E. H., and Virgin, L. N. Stability estimation of high dimensional vibrating systems under state delay feedback control, J. Sound Vibr., 214, 1998, 497-511

[24] Ooi, A. Nikolovska, A., and Manasseh, R., Analysis of time delay effects on a linear bubble chain systema, J. Acous. Soc. Am, (submitted).

[25] Nikolovska, A., Passive Acoustic Transmission and Sound Channelling along Bubbly Chains, PHD Thesis, Department of Mechanical and Manufactoring Eng., The University of Melbourne, 2005,

[26] Nikolovska, A., Ooi, A., and Manasseh, R., On the propagation of acoustic energy in the vicinity of a bubble chain, J. Sound Vibr., 306, 2007, 507523